# Cortical thickness as a contributor to abnormal oscillations in schizophrenia?☆

J. Christopher Edgar [a,*], Yu-Han Chen [b,c], Matthew Lanza [a], Breannan Howell [b,c], Vivian Y. Chow [a], Kory Heiken [a], Song Liu [a], Cassandra Wootton [b,c], Michael A. Hunter [b,c], Mingxiong Huang [d,e], Gregory A. Miller [f], José M. Cañive [b,c]

[a] The Children's Hospital of Philadelphia and University of Pennsylvania, Philadelphia, PA, USA
[b] The University of New Mexico School of Medicine, Department of Psychiatry, Center for Psychiatric Research, Albuquerque, NM, USA
[c] New Mexico Raymond G. Murphy VA Healthcare System, Psychiatry Research, Albuquerque, NM, USA
[d] The University of California San Diego, Department of Radiology, San Diego, CA, USA
[e] San Diego VA Healthcare System, Department of Radiology, San Diego, CA, USA
[f] University of California, Los Angeles, Department of Psychology, USA

## ARTICLE INFO

## ABSTRACT

*Introduction:* Although brain rhythms depend on brain structure (e.g., gray and white matter), to our knowledge associations between brain oscillations and structure have not been investigated in healthy controls (HC) or in individuals with schizophrenia (SZ). Observing function–structure relationships, for example establishing an association between brain oscillations (defined in terms of amplitude or phase) and cortical gray matter, might inform models on the origins of psychosis. Given evidence of functional and structural abnormalities in primary/secondary auditory regions in SZ, the present study examined how superior temporal gyrus (STG) structure relates to auditory STG low-frequency and 40 Hz steady-state activity. Given changes in brain activity as a function of age, age-related associations in STG oscillatory activity were also examined.
*Methods:* Thirty-nine individuals with SZ and 29 HC were recruited. 40 Hz amplitude-modulated tones of 1 s duration were presented. MEG and T1-weighted sMRI data were obtained. Using the sources localizing 40 Hz evoked steady-state activity (300 to 950 ms), left and right STG total power and inter-trial coherence were computed. Time–frequency group differences and associations with STG structure and age were also examined.
*Results:* Decreased total power and inter-trial coherence in SZ were observed in the left STG for initial post-stimulus low-frequency activity (~50 to 200 ms, ~4 to 16 Hz) as well as 40 Hz steady-state activity (~400 to 1000 ms). Left STG 40 Hz total power and inter-trial coherence were positively associated with left STG cortical thickness in HC, not in SZ. Left STG post-stimulus low-frequency and 40 Hz total power were positively associated with age, again only in controls.
*Discussion:* Left STG low-frequency and steady-state gamma abnormalities distinguish SZ and HC. Disease-associated damage to STG gray matter in schizophrenia may disrupt the age-related left STG gamma-band function–structure relationships observed in controls.

## 1. Introduction

Accepting the hypothesis that functional and structural brain measures are more proximal to neurobiological mechanisms and/or pathways associated with schizophrenia (SZ) than overt behavioral measures, it is hoped that neuroimaging-based endophenotypes will identify biological mechanisms at the level of neural circuits (Miller and Rockstroh, 2013; Rasetti and Weinberger, 2011; Rose and Donohoe, 2013). Although brain rhythms depend on brain structure (e.g., gray and white matter), to our knowledge associations between brain oscillations and structure have not been investigated in healthy controls (HC) or in individuals with SZ. Given evidence of functional and structural abnormalities in primary/secondary auditory regions in SZ (reviewed below), and given that gray matter comprises the brain's fundamental units of information processing (neurons), the present study investigated associations between superior temporal gyrus (STG) oscillatory auditory processes and STG gray-matter cortical thickness to begin identifying neural oscillation and brain structure relationships in HC and SZ.

Studies examining evoked auditory measures (averaging brain activity over repetitions of stimuli) show clear evidence of auditory

* Corresponding author at: Department of Radiology, Children's Hospital of Philadelphia, 34th and Civic Center Blvd, Wood Building, Suite 2115, Philadelphia, PA 10104, USA. Tel.: +1 215 590 3573; fax: +1 215 590 1345.
E-mail address: edgarj@email.chop.edu (J.C. Edgar).

abnormalities in SZ (e.g., Rosburg et al., 2008; Smith et al., 2010; Turetsky et al., 2008). The time–frequency profile of neural activity associated with auditory processes in SZ is potentially more informative, as time–frequency analyses provide more detailed information, with abnormalities defined in terms of amplitude or phase abnormalities at a specific frequency in a specific time range (Edgar et al., 2008; Popov et al., 2011). Indeed, electroencephalography (EEG) time–frequency studies have shown that early auditory abnormalities in SZ are best characterized by increased low-frequency trial-to-trial synchrony, observed as decreased phase-locking (PL) in SZ (Blumenfeld and Clementz, 2001; Clementz and Blumenfeld, 2001; Jansen et al., 2004; Johannesen et al., 2005). Using source localization, such abnormalities can be described more precisely. For example, using magnetoencephalography (MEG) and source localization to examine auditory processes in left and right STG in 45 SZ and 45 HC subjects, Edgar et al. (2008) observed that individuals with SZ showed more low-frequency STG phase variability (high theta and alpha bilaterally, low beta left-hemisphere).

A growing literature also shows auditory processing abnormalities in SZ using driving stimuli, and almost all published EEG studies have observed 40 Hz steady-state abnormalities in SZ (Brenner et al., 2003; Hall et al., 2011; Hamm et al., 2012; Hong et al., 2004; Koenig et al., 2012; Krishnan et al., 2009; Kwon et al., 1999; Lenz et al., 2011; Light et al., 2006; Rass et al., 2012; Spencer et al., 2009). MEG steady-state studies applying source localization also show 40 Hz abnormalities in SZ. For example, Teale et al. (2008) observed decreased STG 40 Hz driving inter-trial coherence and evoked activity bilaterally in patients with SZ. In steady-state tasks, the early transient 50 ms and 100 ms auditory responses as well as the steady-state response can be examined (Jacobson and Fitzgerald, 1997; Pantev, 1995). In a recent study comparing early low-frequency and steady-state activity across several driving frequencies, Hamm et al. (2011) found that only low-frequency activity uniquely discriminated groups.

Considering STG structure, reduced STG volume and cortical thickness (CT) are among the most reliably observed structural brain abnormalities in SZ (Ehrlich et al., 2011; Mitelman and Buchsbaum, 2007; Shenton et al., 2001; Smiley et al., 2009). Although brain function and structure are inherently related, associations between STG gray-matter volume and auditory evoked responses have been examined in very few studies of SZ. Using EEG, less left posterior STG and left planum temporale GM were associated with smaller left temporal auditory P300 in SZ (McCarley et al., 1993, 2002). Similar associations were observed between reduced left Heschl's Gyrus GM and smaller Fz mismatch negativity (MMN) in first-episode SZ (Salisbury et al., 2007). Using MEG and examining function–structure associations in each hemisphere, Edgar et al. (2012) observed that in SZ and HC left STG GM was positively associated with left M100 source strength. Although the above studies are of interest, as previously noted auditory abnormalities in SZ are best described as decreased STG low-frequency phase-locking and decreased STG 40 Hz phase-locking for 40 Hz driving stimuli. To our knowledge, however, no study has examined associations between STG time–frequency measures and STG brain structure.

The present study measured associations between left and right STG auditory processes (early transient and 40 Hz steady-state activity) and STG gray matter to begin to assess the structural correlates of oscillatory activity in HC and SZ. Replicating previous studies, it was hypothesized that early low-frequency (~4 to 20 Hz) and sustained 40 Hz driving abnormalities would be observed in SZ. Second, building on studies reporting associations between auditory processes and STG gray matter, it was hypothesized that early low-frequency and sustained 40 Hz driving activity would be associated with STG gray-matter cortical thickness. However, given that STG gray-matter abnormalities in SZ are observed at the onset of the disease (see review by Steen et al., 2006), it was hypothesized that the associations between STG function and structure would be weaker in SZ than in HC, indicating a deterioration of function–structure relationships in SZ. Finally, given that gray-matter cortical thickness decreases with age (Lemaitre et al., 2012),

analyses examined associations between age and STG functional measures.

## 2. Methods and materials

### 2.1. Subjects

Thirty-nine patients with chronic SZ (6 females) and 29 HC (7 females) were recruited. As shown in Table 1, groups did not differ in age or parental socioeconomic status (SES). Patients' SES was lower than controls', and patients were slightly less educated than controls. Patients' mean total scores on the Positive and Negative Syndrome Scale (PANSS) (Kay et al., 1987) were 17.79 for positive symptoms and 15.79 for negative symptoms. Recruitment procedures and information on inclusion and exclusion criteria are reported in Smith et al. (2010); there is no overlap in the subjects reported in Smith et al. and this study.

Five HC and 2 SZ were left-handed as assessed by the Waterloo Handedness Questionnaire (Bryden, 1977). Patients with SZ were medicated and clinically stable without change in medications for at least three months before MEG. In the patient group, 28 subjects were treated with 2nd generation antipsychotics, four subjects were treated with the 1st generation antipsychotic haloperidol, five subjects treated with more than one antipsychotic, and two subjects were not taking medications. Thirteen subjects with SZ and 7 HC were smokers.

### 2.2. Steady-state task

The amplitude of a 500 Hz stimulus was modulated at 40 Hz. Stimuli of 1 s duration were binaurally presented with a 4 s ISI ($\pm 2$ s) through earphones placed in each ear canal. For each ear, the peak intensity of the click was presented 35 dB above each subject's hearing threshold. The number of steady-state stimuli presented depended on the MEG recording time available. MEG data were examined only from subjects with $50+$ trials. The mean number of trials in the control group (range 51 to 125, mean = 84) and the SZ group (range 58 to 113 mean = 79) did not differ ($t(66) = 1.11$, $p = 0.27$).

### 2.3. Structural magnetic resonance imaging (sMRI)

T1-weighted MPRAGE structural MR images were collected on a Siemens 3T TIM Trio scanner at the Mind Research Network (MRN). Images were collected with a field-of-view (FOV) = 256 × 256 mm, 192 sagittal slices, and 1 × 1 × 1 mm spatial resolution. This was a five-echo sequence with echo times (TE) of 1.64, 3.5, 5.36, 7.22, and 9.08 ms, a repetition time (TR) = 2530 ms, a gray-white matter contrast enhancement inversion recovery time (TI) of 1200 ms, and 7° flip angle.

### 2.4. MEG, EEG, and sMRI data acquisition and coregistration

MEG data were recorded in a magnetically shielded room (Vacuumschmelze, Germany) using all channels of a 306-channel Vector-View MEG system (Elekta-Neuromag, Helsinki, Finland). After

**Table 1**
Demographic information (SES measures missing from a few subjects).

|  | HC (N = 29) | | SZ (N = 39) | |
|---|---|---|---|---|
|  | Mean | SD | Mean | SD |
| Age | 37.90 | 10.88 | 40.87 | 12.62 |
| Education (years) | 14.58 | 1.52 | 13.15 | 2.16 |
| SES | 53.04 | 16.10 | 65.51 | 10.66 |
| Parental SES | 39.69 | 18.18 | 48.30 | 17.64 |

HC had higher SES, $t(61) = 3.70$, and more education, $t(66) = 3.05$ ($ps < 0.01$). Group differences in age, $t(66) = 1.02$, and parental SES, $t(55) = -1.80$, were not significant ($ps > 0.05$).

a band-pass filter (0.1–330 Hz), MEG signals were digitized at 1000 Hz. EEG data were recorded from 60 equidistant sites (Falk Minow Customized Easy Cap®). The left mastoid served as the EEG reference. Comparisons between EEG and MEG will be presented in a separate paper. Electro-oculogram (EOG) (vertical EOG on the upper and lower left sides) and electrocardiogram (ECG) (at the collarbone) were also obtained.

To coregister MEG and sMRI data, three anatomical landmarks (nasion and right and left preauriculars) as well as an additional 200 + points on the scalp and face were digitized for each subject using the Probe Position Identification (PPI) System (Polhemus, Colchester, VT). During the MEG recording, the subject's head position was monitored using four HPI coils attached to the scalp. To co-register the MEG and sMRI for each subject, the three fiducials were identified in the subject's sMRI, and a transformation matrix that involved rotation and translation between the MEG and sMRI coordinate systems was obtained by matching the 200 + points from the PPI measurements to the surface of the scalp and face from the sMRI using BrainVoyager QX (Brain Innovations, The Netherlands).

### 2.5. Magnetic source analysis

MEG raw signals were first processed with Signal Space Separation (SSS; Taulu et al., 2004) using Maxfilter (Elekta MaxfilterTM; Elekta Oy). SSS separates neuronal magnetic signals arising from inside the MEG sensor array from external magnetic signals arising from the surrounding environment to effectively reduce environmental noise and artifacts. Following SSS, eye-blink activity was corrected using the methods outlined in Berg and Scherg (1994). Epochs with artifacts other than blinks were rejected by amplitude and gradient criteria (amplitude > 1200fT/cm, gradient > 800fT/cm/sample).

Source localization and scoring were done blind to group. For source localization analyses, artifact-free epochs −400 ms pre-stimulus to 1000 ms post-stimulus were defined from the continuous recording. Noncontaminated epochs were averaged, and a 40 Hz (width 20 Hz) band-pass filter applied. Determination of the location of the 40 Hz steady-state generators in the left and right hemispheres was accomplished by fitting a dipole source in each hemisphere using a realistic head model. For modeling the 40 Hz steady-state response, data 300 to 950 ms post-stimulus were selected. Left- and right-hemisphere responses were separately localized, with the MEG channels on the opposite hemisphere turned off. In 4 HC and 5 SZ the left STG 40 Hz response was not well localized (source strength less than 5 nA-m, or location >15 mm from Heschl's Gyrus). In 1 SZ the right STG 40 Hz was not well localized. In these subjects, the 'missing' STG response was fixed at the analog of the localized contralateral response, with the 'missing' STG dipole oriented to optimally explain the variance in the 40 Hz response. Examining the full model (left + right STG sources + eye-blink source), goodness-of-fit values (300 to 950 ms period) for HC (mean = 78%, SD = 10.15) and SZ (mean = 76%, SD = 12.0) did not differ, $t(66) = 0.74$, n.s.

### 2.6. Source time–frequency analysis

The calculation of single-trial phase and magnitude for the left and right STG sources used procedures outlined in Hoechstetter et al. (2004) where in each subject the derived source model was applied to the raw unfiltered data. Transformation from the time domain to the time–frequency domain used complex demodulation procedures (Papp and Ktonas, 1977) implemented in BESA 5.3, using frequencies between 4 and 60 Hz, in steps of 2 Hz. Continuous data were analyzed relative to tone onset every 25 ms (i.e., each 40 Hz cycle), utilizing ± 39.4 ms and ± 2.83 Hz (full width at half maximum parameters) of contiguous data at each 25 ms step.

Total power and phase-locking measures were extracted from the single-trial complex time–frequency matrix. Total power is calculated by averaging the time–frequency spectra of each MEG epoch. When baseline power is subtracted, poststimulus total power assesses the poststimulus increase in the magnitude/power of oscillatory activity (temporal spectral evolution, TSE). A measure of phase-locking referred to as inter-trial coherence was computed as $abs\left(\frac{1}{N}\sum_{k=1}^{N}e^{i\phi(k)}\right)$ where the sum is over all $N$ trials, and $\phi(k)$ is the phase of the signal at each time frequency bin (see below) in the $k$th trial. Inter-trial coherence (ITC) is a normalized measure with ITC = 1 reflecting no phase variability and ITC = 0 reflecting maximal phase variability across trials.

For all analyses involving time–frequency measures (i.e., $t$-tests and correlations), a clustering method controlled family-wise error (e.g., see Edgar et al., 2008, 2013). The method computes the probability of a random field of noise producing a cluster of adjacent time–frequency cells of a given size after the noise is thresholded at a given probability level and provides a corrected $p$-value. The cluster size needed to obtain the desired family-wise correction was determined using a standard fMRI package (AFNI AlphaSim) and clustering performed with custom MatLab software. For all analyses, subjects more than 2.5 standard deviations were excluded (typically 1 to 2 subjects per analysis).

### 2.7. Cortical thickness measures

FreeSurfer uses intensity and continuity sMRI information in segmentation and deformation procedures to obtain cortical thickness (CT) measures, calculated as the closest distance from the gray/white to gray/cerebral-spinal-fluid boundary at each vertex on the tessellated surface (Fischl and Dale, 2000). Using the FreeSurfer software suite (http://sufer.nmr.mgh.harvard.ed), the sMRI from each subject were processed to obtain STG CT measures using the procedures outlined in Edgar et al. (2012).

The present study examined gray-matter CT, as CT may represent a particularly reliable endophenotype for SZ (Ehrlich et al., 2011), given that alterations of CT reflect pathological abnormalities such as reduced neuropil density or loss of glial cells (Stark et al., 2004), abnormalities observed in postmortem SZ studies (Glantz et al., 2006; Kubota et al., 2011). In addition, genetic studies have suggested a heritability component for CT loss but not for volume in SZ (Goghari et al., 2007; Gogtay et al., 2007; Goldman et al., 2009; Winkler et al., 2010).

For analyses involving STG CT, to reduce the chance of type I error in each hemisphere a composite score was calculated, with each STG subregion score scaled by its surface area (SA).

STG GM composite measure

$$= \frac{(HG\ SA) \times (HG\ CT) + (PT\ SA) \times (PT\ CT) + (LA\ SA) \times (LA\ CT)}{(HG\ SA) + (PT\ SA) + (LA\ SA)}$$

## 3. Results

### 3.1. Source localization analyses

ANOVAs assessed Hemisphere and Group differences in the position of the STG 40 Hz steady-state dipoles (excluding the 4 HC and 6 SZ subjects whose 'missing' STG dipole was placed at the analog of the contralateral response). Examining medial-to-lateral position (x axis), a main effect of Group, $F(1,56) = 4.47$, $p = 0.04$, indicated more medial STG sources in patients than controls (~2 mm). Examining anterior-to-posterior position (y axis), a main effect of Hemisphere, $F(1,56) = 99.37$, $p < 0.001$, indicated more anterior right than left STG sources in both groups. Examining inferior-to-superior position (z axis), neither of the main effects nor the interaction was significant.

### 3.2. Total power analyses

Fig. 1 shows total-power family-wise corrected statistical maps (HC > SZ blue, SZ > HC red). In the left STG, statistical maps show (1) greater pre-stimulus ~4 to 20 Hz power in SZ than HC (Cohen's $D = 0.96$), (2) greater post-stimulus ~4 to 12 Hz power in HC than SZ from ~25 to 150 ms (Cohen's $D = 0.89$), and (3) greater 40 Hz steady-state activity in HC than SZ from ~500 to 1000 ms (Cohen's $D = 0.53$). Insets show left STG post-stimulus low-frequency (4 to 12 Hz activity averaged from 25 to 150 ms) and 40 Hz steady-state (38 to 42 Hz activity averaged from 300 to 950 ms) total power values for each subject. In the right STG, statistical maps show less ~4 to 12 Hz de-synchronization in SZ than in HC from ~700 to 900 ms (Cohen's $D = 0.61$).

### 3.3. ITC analyses

Fig. 2 shows ITC family-wise corrected statistical maps (HC > SZ blue, SZ > HC red). In the left STG, statistical maps show (1) greater post-stimulus ~4 to 12 Hz ITC in HC than SZ from ~25 to 300 ms (Cohen's $D = 0.69$) and (2) greater 40 Hz steady-state ITC in HC than SZ from ~400 to 1000 ms (Cohen's $D = 0.65$). Insets show left STG post-stimulus low-frequency (4 to 12 Hz activity averaged from 25 to 300 ms) and 40 Hz steady-state (38 to 42 Hz activity averaged from 300 to 950 ms) ITC values for each subject. In the right STG, statistical maps show greater early ~50 Hz ITC in HC than SZ from ~25 to 200 ms (Cohen's $D = 0.76$).

### 3.4. Associations between STG gray-matter cortical thickness and STG total power and ITC

A Group by Hemisphere ANOVA on STG gray-matter CT showed a marginally significant main effect of Group (HC > SZ), $F(1,66) = 3.20$, $p = 0.08$.

Fig. 3 shows family-wise corrected statistical maps of correlations between STG gray-matter CT and left STG total power (upper panel) and ITC (lower panel) for each group (right hemisphere not shown, as significant correlations were observed only in the left hemisphere). Insets show scatterplots of gray-matter CT versus 40 Hz steady-state ITC and total power (38 to 42 Hz activity averaged from 300 to 950 ms) for each group. Insets show that increased gray-matter CT was associated with increased 40 Hz steady-state total power and ITC in HC ($ps < 0.05$) but not SZ ($ps > 0.05$).

### 3.5. Associations between age and STG total power and ITC

Fig. 4 shows family-wise corrected statistical maps of correlations between age and left STG total power (upper panel) and ITC (lower panel) for each group (right hemisphere not shown, as significant correlations were observed only in the left hemisphere). Insets show scatterplots of age versus left STG low-frequency (4 to 16 Hz activity averaged from 25 to 150 ms) and 40 Hz ITC and total power (38 to 42 Hz activity averaged from 300 to 950 ms) for each group. Insets show that increased age was associated with decreased early low-frequency total power and ITC as well as decreased 40 Hz steady-state total power and ITC in HC ($ps < 0.05$) but not SZ ($ps > 0.05$).

## 4. Discussion

Present findings indicated multiple disruptions to STG auditory areas in SZ. First, replicating earlier studies, analyses showed STG low-frequency and 40 Hz steady-state total power and ITC abnormalities in SZ. Second, STG function–structure relationships were observed only in HC, with STG gray-matter CT accounting for ~13% of the variance in STG 40 Hz steady-state total power and ~16% of the variance in 40 Hz steady-state ITC. Finally, in controls only, associations with age were observed, with decreased left STG low-frequency and 40 Hz steady-state total power and ITC observed in older controls.

Examining gray-matter changes associated with normal aging, Pakkenberg and Gundersen (1997) estimated a loss of ~85,000 neurons per day (from an estimated ~20 billion total neocortical neurons). As reviewed in Raz and Rodrigue (2006), age-related gray-matter changes associated with normal aging include (but are not limited to) myelin pallor, loss of neuronal bodies in the neocortex, shrinkage and dysmorphology of neurons, reduction in synaptic density, deafferentation, loss of dendritic spines, reduction in DNA repair ability, and failure to remove neurons with damaged nuclear DNA. Present findings indicate that in HC these age-related STG gray-matter changes are associated with weaker and less synchronous auditory responses.
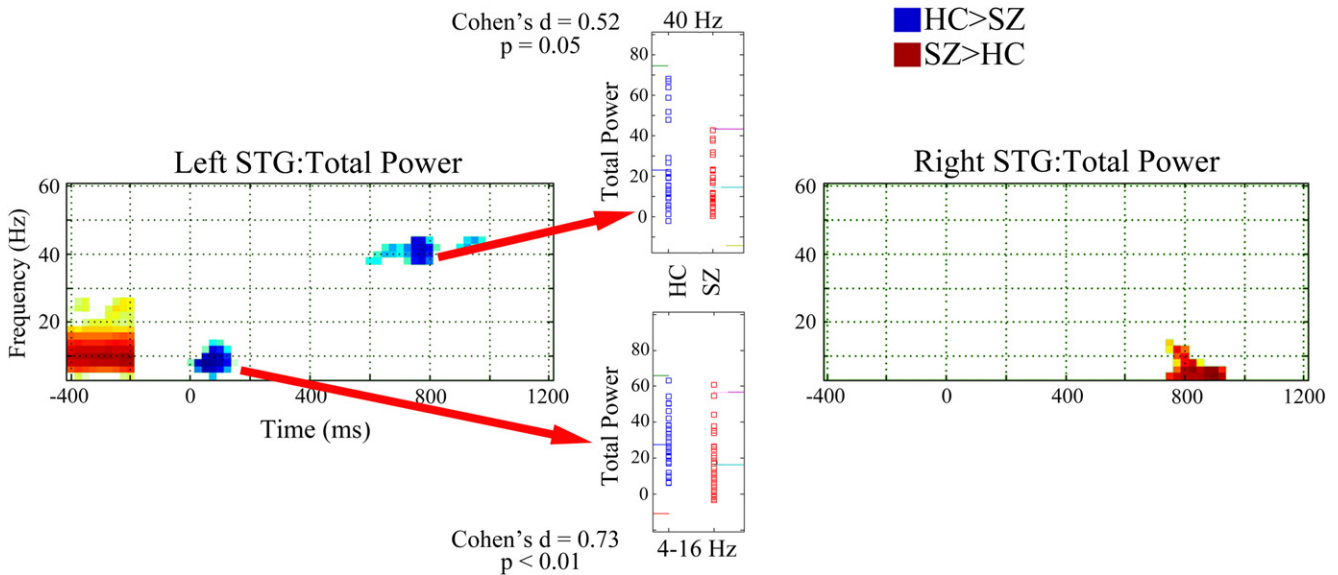


**Fig. 1.** Total power family-wise corrected statistical maps for left and right STG (HC > SZ blue, SZ > HC red). Time is shown on the x axis and frequency on the y axis. The −400 to −200 ms period shows pre-stimulus total power without baseline subtraction. Insets show left STG post-stimulus low-frequency (4 to 12 Hz activity averaged from 25 to 150 ms) and 40 Hz steady-state (38 to 42 Hz activity averaged from 300 to 950 ms) total power values for each subject. In the inset, for each measure, colored lines show the mean and ±2 SD.
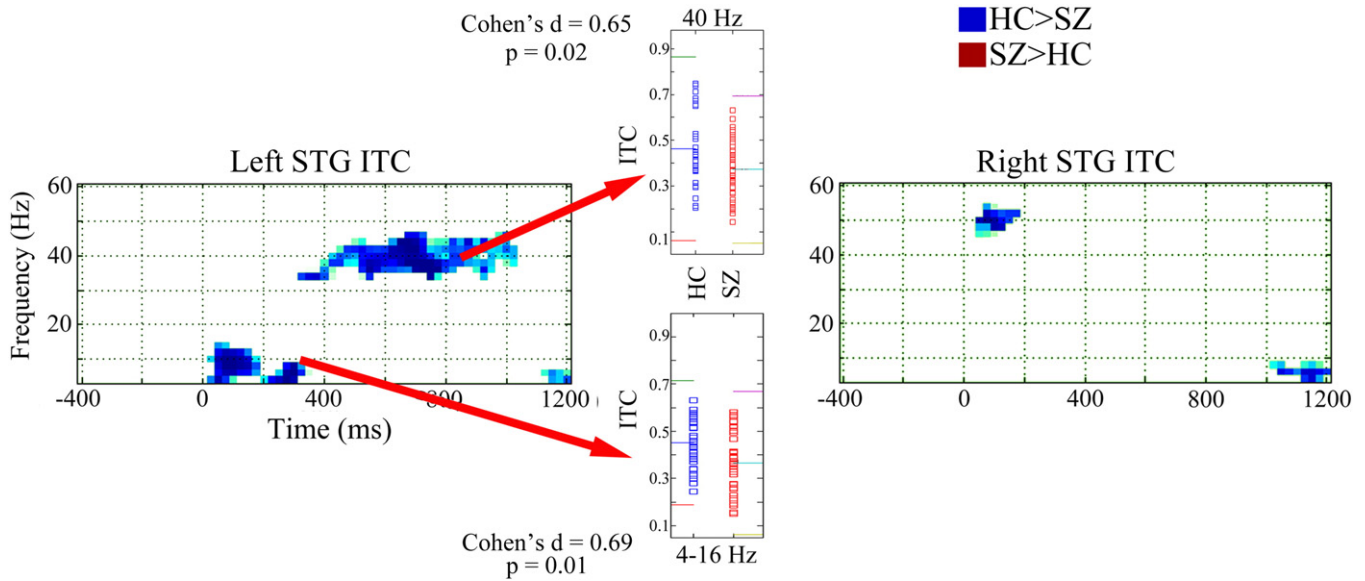
**Fig. 2.** Inter-trial coherence family-wise corrected statistical maps for left and right STG (HC > SZ blue, SZ > HC red). Time is shown on the x axis and frequency on the y axis. Insets show left STG post-stimulus low-frequency (4 to 12 Hz activity averaged from 25 to 150 ms) and 40 Hz steady-state (38 to 42 Hz activity averaged from 300 to 950 ms) inter-trial coherence values for each subject. In the inset, for each measure, colored lines show the mean and ±2 SD.

We hypothesize that individuals with SZ do not show 40 Hz activity, age, and gray-matter associations because gray-matter abnormalities in SZ differ from the gray-matter changes observed in normal aging, with gray-matter loss in SZ prior to or at the onset of the disease (Jung et al., 2012; Steen et al., 2006) precluding normal age-related function–structure associations. For example, in typical adult-onset schizophrenia the extent of annualized progressive brain tissue loss is estimated to be 0.5%, more than twice the rate of controls

(Hulshoff Pol and Kahn, 2008). In addition, likely different from the age-related gray-matter changes in HC, in SZ gray-matter reductions are thought to be primarily due to elimination of the neuropil between neuron bodies (the reduced neuropil hypothesis) (Selemon and Goldman-Rakic, 1999). Sweet et al. (2003) found that, within auditory cortex, mean somal volumes of deep layer 3 pyramidal cells in BA 41 and 42 were reduced in SZ, and Sweet et al. (2007) observed reduced axon terminal densities in feed-forward auditory pathways. A combined
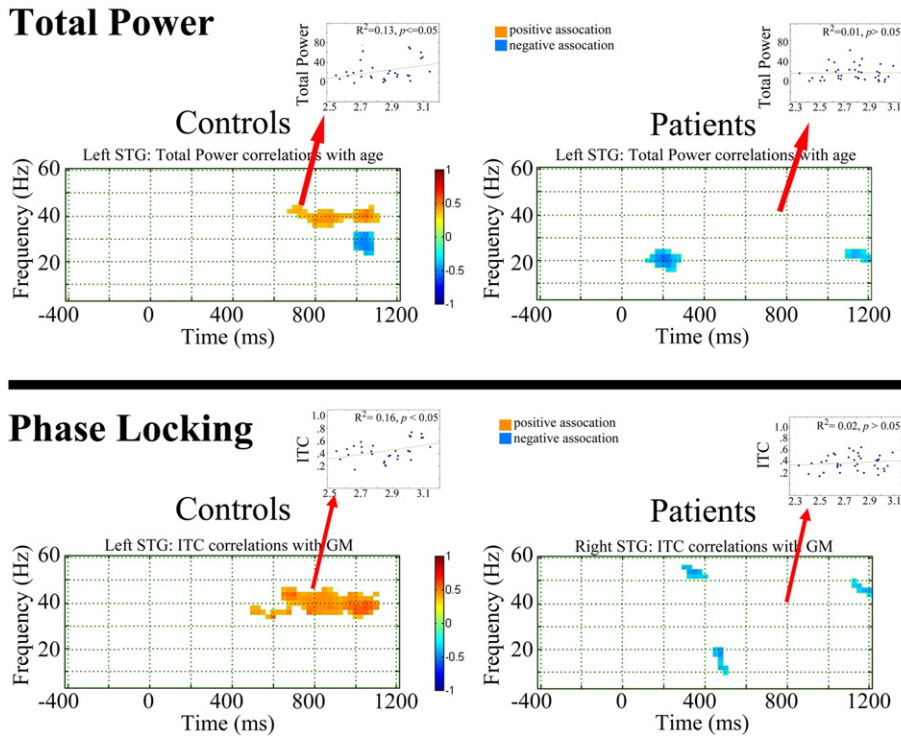


**Fig. 3.** Family-wise corrected statistical maps showing correlations between gray-matter cortical thickness and left STG total power (upper panel) and ITC (lower panel) for each group. Time is shown on the x axis and frequency on the y axis. Insets show scatterplots of gray-matter cortical thickness versus left STG low-frequency (4 to 16 Hz activity averaged from 25 to 150 ms) and 40 Hz ITC and total power (38 to 42 Hz activity averaged from 300 to 950 ms) for each group, with the $R^2$ values showing the percent variance explained.

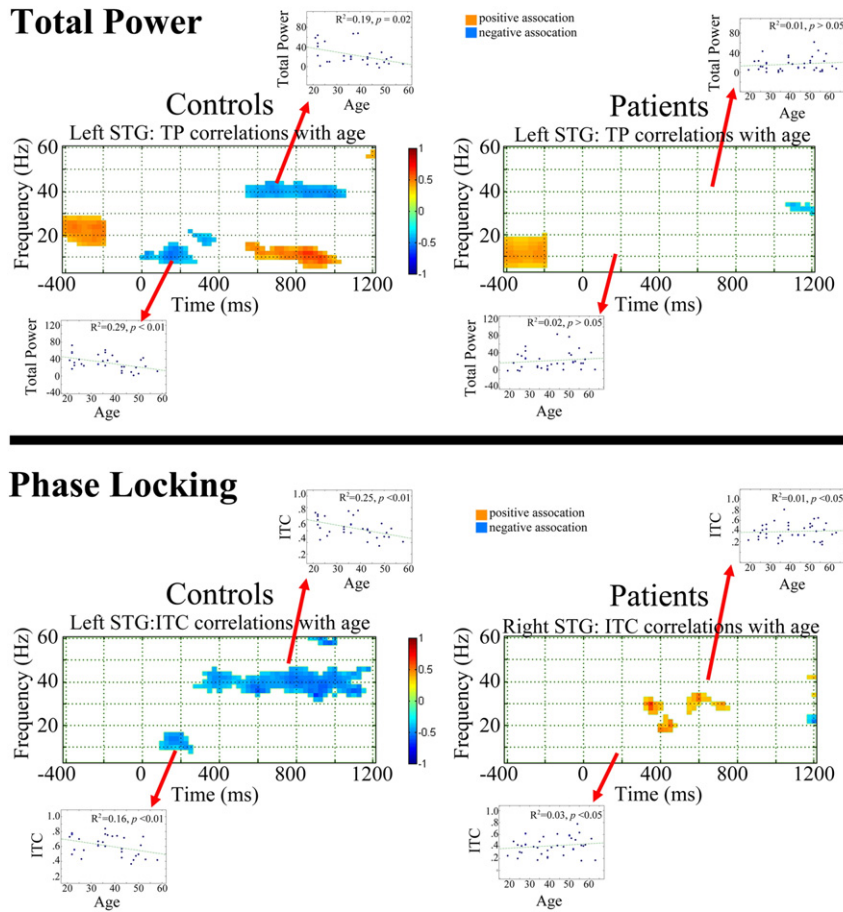## Time-frequency Associations with Age



**Fig. 4.** Family-wise corrected statistical maps showing correlations between age and left STG total power (upper panel) and ITC (lower panel) for each group. Time is shown on the x axis and frequency on the y axis. The −400 to −200 ms period shows pre-stimulus total power without baseline subtraction. Insets show scatterplots of age versus left STG low-frequency (4 to 16 Hz activity averaged from 25 to 150 ms) and 40 Hz ITC and total power (38 to 42 Hz activity averaged from 300 to 950 ms) for each group, with the $R^2$ values showing the percent variance explained.

MEG and proton magnetic resonance spectroscopy study showed that the number and integrity of neurons (assessed via auditory cortex N-acetylaspartate) and the density and functional integrity of cell membranes (assessed via auditory cortex choline-containing compounds) are associated with M100 source strength (Soros et al., 2006).

Failure to observe a structure–function association in SZ may also be due to heterogeneity in the present SZ group. In a recent review, Moran et al. (2013) noted (1) the likely influence of individual genetic polymorphisms on cortical gray matter in SZ (e.g., the association of COMT Val/Val genotype with increased age-associated gray-matter loss in childhood-onset SZ reported in Raznahan et al. (2011)), and (2) evidence indicating that gray-matter loss in SZ is associated with genetic risk, with the rate of age-related gray matter loss in individual with SZ at least 50% due to genes implicated in SZ (e.g., see Brans et al., 2008). The above suggest that the present group-level analyses showing a loss of function–structure and age relationships in SZ may 'overestimate' this loss, with function–structure relationships perhaps existing in some individuals with SZ but reduced in others. Given the Moran et al. findings, studies examining function–structure associations in SZ subgroups (e.g., different COMT genotypes) as well as function–structure processes in monozygotic and dizygotic twin pairs are of interest. Longitudinal studies are also needed to more fully examine how STG function–structure processes change over time in HC and SZ.

A few other findings are of note. First, pre-stimulus low-frequency activity as well as post-stimulus low-frequency activity was were

associated with age but not gray matter, suggesting that the sustained 40 Hz response is more dependent on the integrity of local neural networks than is the early low-frequency response. It is hypothesized that this reflects differences in the neural networks sustaining low-frequency versus 40 Hz steady-state activity. Specifically, whereas local networks of pyramidal cells and inhibitory interneurons in the superficial cortical layers are likely sufficient to maintain the 40 Hz driving response, low-frequency activity, associated with the 50 ms and 100 ms auditory responses, likely reflects input to primary/secondary auditory areas via thalamocortical interactions in the deep cortical layers as well as interactions between temporal and frontal areas (Buffalo et al., 2011; Chen et al., 2013; Knight et al., 1999). An emerging hypothesis suggests that the multiple abnormalities observed in layer 3 inhibitory interneuron parvalbumin basket cell GABAergic neurons and pyramidal cell networks in SZ are a homeostatic response to a more fundamental abnormality in SZ — decreased layer 3 pyramidal cell dendritic spine density (for a review, see Lewis et al., 2012). A STG dendritic spine density deficit in SZ (thus indicating reduced glutamatergic synapses onto pyramidal cells) could account for the gamma oscillatory abnormalities observed in the present study. Finding consistent with this include post-mortem studies observing that STG pyramidal cells in SZ are smaller have and have lower spine density (Sweet et al., 2004, 2009).

Second, as shown in Fig. 3, increased background activity was observed in individuals with SZ in the left and right STG. Group differences

were observed primarily for frequencies less than 30 Hz. Thus, although this finding is consistent with the hypothesis of increased background noise in SZ (Gandal et al., 2012), present findings suggest that in STG regions this abnormality is observed only in theta to beta bands. The increased low-frequency pre-stimulus activity in SZ suggests a reduced ability to return to (or perhaps maintain) typical STG baseline activity, thus perhaps resulting in an inability to fully engage local neural populations at stimulus onset. Present results are similar to recent findings by Hong et al. (2012), where increased low-frequency resting as well as pre-stimulus activity was observed in SZ than HC.

Third, in the right STG, group differences were observed in the early transient 40 Hz response (i.e., between 25 and 200 ms). Transient auditory evoked gamma group differences have been reported in some but not all studies (Roach and Mathalon, 2008). Discrepancies in EEG studies may be due to examining the composite response at midline electrodes rather than separately examining left and right STG activity. However, studies using MEG to examine left and right hemisphere activity have not observed early 40 Hz group differences, suggesting that early auditory gamma-band abnormalities are not a robust finding in SZ.

The present study has several limitations. First, most subjects were chronic patients, with almost all patients on medication. As such, it is not possible to determine whether the observed abnormalities were due to the disorder or an effect of medication. Studies, however, show that 40 Hz steady-state abnormalities in SZ are present at first onset and in first-degree relatives (Rass et al., 2012; Spencer et al., 2008), suggesting that 40 Hz steady-state abnormalities in SZ are not due to medication. In addition, in a review of 100 ms auditory studies Rosburg et al. (2008) concluded that medication did not seem to account for group differences in N100 activity. Second, although consistent with all other previous studies observing relationships between auditory responses and left but not right STG gray matter (Edgar et al., 2012; McCarley et al., 1993, 2002), it remains unclear why the associations in the present study were observed only in the left hemisphere. Finally, to more fully understand auditory time–frequency abnormalities in SZ as well as oscillatory processes in controls, studies are needed to identify other brain measures that predict oscillatory activity. For example, Roberts et al. (2009) showed that acoustic radiations white matter predicts STG auditory latencies in typically developing children, and Gaetz et al. (2011) showed that magnetic resonance spectroscopy GABA levels predict gamma activity in motor cortex. Studies examining associations between STG time–frequency measures with acoustic radiations white matter and local GABA are needed. Given the multiple determinates of oscillatory activity, just as SZ is a heterogeneous disorder, it may turn out that neuroimaging-based endophenotypes are similarly complex, with a combination of gray matter, white matter, and neurochemical measures best predicting oscillatory abnormalities in SZ.

In sum, present findings replicate studies showing that early left STG low-frequency and 40 Hz steady-state auditory abnormalities distinguish SZ and HC populations. Damage to STG gray matter at the onset of schizophrenia may disrupt the normal age-related left STG function–structure relationships observed in controls.

## Acknowledgments

## Declaration of interest

The authors have no conflicts of interest to report.

## References

Berg, P., Scherg, M., 1994. A multiple source approach to the correction of eye artifacts. Electroencephalogr. Clin. Neurophysiol. 90 (3), 229–241.

Blumenfeld, L.D., Clementz, B.A., 2001. Response to the first stimulus determines reduced auditory evoked response suppression in schizophrenia: single trials analysis using MEG. Clin. Neurophysiol. 112 (9), 1650–1659.

Brans, R.G., van Haren, N.E., van Baal, G.C., Schnack, H.G., Kahn, R.S., Hulshoff Pol, H.E., 2008. Heritability of changes in brain volume over time in twin pairs discordant for schizophrenia. Arch. Gen. Psychiatry 65 (11), 1259–1268.

Brenner, C.A., Sporns, O., Lysaker, P.H., O'Donnell, B.F., 2003. EEG synchronization to modulated auditory tones in schizophrenia, schizoaffective disorder, and schizotypal personality disorder. Am. J. Psychiatry 160 (12), 2238–2240.

Bryden, M.P., 1977. Measuring handedness with questionnaires. Neuropsychologia 15 (4–5), 617–624.

Buffalo, E.A., Fries, P., Landman, R., Buschman, T.J., Desimone, R., 2011. Laminar differences in gamma and alpha coherence in the ventral stream. Proc. Natl. Acad. Sci. U. S. A. 108 (27), 11262–11267.

Chen, Y., Edgar, J.C., Huang, M., Hunter, M.A., Epstein, E., Howell, B., et al., 2013. Frontal and superior temporal auditory processing abnormalities in schizophrenia. NeuroImage 2, 695–702.

Clementz, B.A., Blumenfeld, L.D., 2001. Multichannel electroencephalographic assessment of auditory evoked response suppression in schizophrenia. Exp. Brain Res. 139 (4), 377–390.

Edgar, J.C., Hanlon, F.M., Huang, M.X., Weisend, M.P., Thoma, R.J., Carpenter, B., et al., 2008. Superior temporal gyrus spectral abnormalities in schizophrenia. Psychophysiology 45 (5), 812–824.

Edgar, J.C., Hunter, M.A., Huang, M., Smith, A.K., Chen, Y., Sadek, J., et al., 2012. Temporal and frontal cortical thickness associations with M100 auditory activity and attention in healthy controls and individuals with schizophrenia. Schizophr. Res. 140 (1–3), 250–257.

Edgar, J.C., Khan, S.Y., Blaskey, L., Chow, V.Y., Rey, M., Gaetz, W., Cannon, K.M., Monroe, J.F., Cornew, L., Qasmieh, S., Liu, S., Welsh, J.P., Levy, S.E., Roberts, T.P., 2013. Neruomagnetic noise predicts evoked-response delays and core language deficits in autism spectrum disorders. J. Autism Dev. Disord.

Ehrlich, S., Yendiki, A., Greve, D.N., Manoach, D.S., Ho, B.C., White, T., et al., 2011. Striatal function in relation to negative symptoms in schizophrenia. Psychol. Med. 1–16.

Fischl, B., Dale, A.M., 2000. Measuring the thickness of the human cerebral cortex from magnetic resonance images. Proc. Natl. Acad. Sci. U. S. A. 97 (20), 11050–11055.

Gaetz, W., Edgar, J.C., Wang, D.J., Roberts, T.P., 2011. Relating MEG measured motor cortical oscillations to resting gamma-aminobutyric acid (GABA) concentration. NeuroImage 55 (2), 616–621.

Gandal, M.J., Edgar, J.C., Klook, K., Siegel, S.J., 2012. Gamma synchrony: towards a translational biomarker for the treatment-resistant symptoms of schizophrenia. Neuropharmacology 62 (3), 1504–1518.

Glantz, L.A., Gilmore, J.H., Lieberman, J.A., Jarskog, L.F., 2006. Apoptotic mechanisms and the synaptic pathology of schizophrenia. Schizophr. Res. 81 (1), 47–63.

Goghari, V.M., Rehm, K., Carter, C.S., MacDonald, A.W., 2007. Sulcal thickness as a vulnerability indicator for schizophrenia. Br. J. Psychiatry 191, 229–233.

Gogtay, N., Greenstein, D., Lenane, M., Clasen, L., Sharp, W., Gochman, P., et al., 2007. Cortical brain development in nonpsychotic siblings of patients with childhood-onset schizophrenia. Arch. Gen. Psychiatry 64 (7), 772–780.

Goldman, A.L., Pezawas, L., Mattay, V.S., Fischl, B., Verchinski, B.A., Chen, Q., et al., 2009. Widespread reductions of cortical thickness in schizophrenia and spectrum disorders and evidence of heritability. Arch. Gen. Psychiatry 66 (5), 467–477.

Hall, M.H., Taylor, G., Sham, P., Schulze, K., Rijsdijk, F., Picchioni, M., et al., 2011. The early auditory gamma-band response is heritable and a putative endophenotype of schizophrenia. Schizophr. Bull. 37 (4), 778–787.

Hamm, J.P., Gilmore, C.S., Picchetti, N.A., Sponheim, S.R., Clementz, B.A., 2011. Abnormalities of neuronal oscillations and temporal integration to low- and high-frequency auditory stimulation in schizophrenia. Biol. Psychiatry 69 (10), 989–996.

Hamm, J.P., Gilmore, C.S., Clementz, B.A., 2012. Augmented gamma band auditory steady-state responses: support for NMDA hypofunction in schizophrenia. Schizophr. Res. 138 (1), 1–7.

Hoechstetter, K., Bornfleth, H., Weckesser, D., Ille, N., Berg, P., Scherg, M., 2004. BESA source coherence: a new method to study cortical oscillatory coupling. Brain Topogr. 16 (4), 233–238.

Hong, L.E., Summerfelt, A., McMahon, R., Adami, H., Francis, G., Elliott, A., et al., 2004. Evoked gamma band synchronization and the liability for schizophrenia. Schizophr. Res. 70 (2–3), 293–302.

Hong, L.E., Summerfelt, A., Mitchell, B.D., O'Donnell, P., Thaker, G.K., 2012. A shared low-frequency oscillatory rhythm abnormality in resting and sensory gating in schizophrenia. Clin. Neurophysiol. 123 (2), 285–292.

Hulshoff Pol, H.E., Kahn, R.S., 2008. What happens after the first episode? A review of progressive brain changes in chronically ill patients with schizophrenia. Schizophr. Bull. 34 (2), 354–366.

Jacobson, G.P., Fitzgerald, M.B., 1997. Auditory evoked gamma band potential in normal subjects. J. Am. Acad. Audiol. 8 (1), 44–52.

Jansen, B.H., Hegde, A., Boutros, N.N., 2004. Contribution of different EEG frequencies to auditory evoked potential abnormalities in schizophrenia. Clin. Neurophysiol. 115 (3), 523–533.

Johannesen, J.K., Kieffaber, P.D., O'Donnell, B.F., Shekhar, A., Evans, J.D., Hetrick, W.P., 2005. Contributions of subtype and spectral frequency analyses to the study of P50 ERP amplitude and suppression in schizophrenia. Schizophr. Res. 78 (2–3), 269–284.

Jung, W.H., Borgwardt, S., Fusar-Poli, P., Kwon, J.S., 2012. Gray matter volumetric abnormalities associated with the onset of psychosis. Front. Psychiatry/Front. Res. Found. 3, 101.

Kay, S.R., Fiszbein, A., Opler, L.A., 1987. The positive and negative syndrome scale (PANSS) for schizophrenia. Schizophr. Bull. 13 (2), 261–276.

Knight, R.T., Staines, W.R., Swick, D., Chao, L.L., 1999. Prefrontal cortex regulates inhibition and excitation in distributed neural networks. Acta Psychol. 101 (2–3), 159–178.

Koenig, T., van Swam, C., Dierks, T., Hubl, D., 2012. Is gamma band EEG synchronization reduced during auditory driving in schizophrenia patients with auditory verbal hallucinations? Schizophr. Res. 141 (2–3), 266–270.

Krishnan, G.P., Hetrick, W.P., Brenner, C.A., Shekhar, A., Steffen, A.N., O'Donnell, B.F., 2009. Steady state and induced auditory gamma deficits in schizophrenia. NeuroImage 47 (4), 1711–1719.

Kubota, M., Miyata, J., Yoshida, H., Hirao, K., Fujiwara, H., Kawada, R., et al., 2011. Age-related cortical thinning in schizophrenia. Schizophr. Res. 125 (1), 21–29.

Kwon, J.S., O'Donnell, B.F., Wallenstein, G.V., Greene, R.W., Hirayasu, Y., Nestor, P.G., et al., 1999. Gamma frequency-range abnormalities to auditory stimulation in schizophrenia. Arch. Gen. Psychiatry 56 (11), 1001–1005.

Lemaitre, H., Goldman, A.L., Sambataro, F., Verchinski, B.A., Meyer-Lindenberg, A., Weinberger, D.R., et al., 2012. Normal age-related brain morphometric changes: non-uniformity across cortical thickness, surface area and gray matter volume? Neurobiol. Aging 33 (3), 617 (e1-9).

Lenz, D., Fischer, S., Schadow, J., Bogerts, B., Herrmann, C.S., 2011. Altered evoked gamma-band responses as a neurophysiological marker of schizophrenia? Int. J. Psychophysiol. 79 (1), 25–31.

Lewis, D.A., Curley, A.A., Glausier, J.R., Volk, D.W., 2012. Cortical parvalbumin interneurons and cognitive dysfunction in schizophrenia. Trends Neurosci. 35 (1), 57–67.

Light, G.A., Hsu, J.L., Hsieh, M.H., Meyer-Gomes, K., Sprock, J., Swerdlow, N.R., et al., 2006. Gamma band oscillations reveal neural network cortical coherence dysfunction in schizophrenia patients. Biol. Psychiatry 60 (11), 1231–1240.

McCarley, R.W., Shenton, M.E., O'Donnell, B.F., Faux, S.F., Kikinis, R., Nestor, P.G., et al., 1993. Auditory P300 abnormalities and left posterior superior temporal gyrus volume reduction in schizophrenia. Arch. Gen. Psychiatry 50 (3), 190–197.

McCarley, R.W., Salisbury, D.F., Hirayasu, Y., Yurgelun-Todd, D.A., Tohen, M., Zarate, C., et al., 2002. Association between smaller left posterior superior temporal gyrus volume on magnetic resonance imaging and smaller left temporal P300 amplitude in first-episode schizophrenia. Arch. Gen. Psychiatry 59 (4), 321–331.

Miller, G.A., Rockstroh, B., 2013. Endophenotypes in psychopathology research: where do we stand? Annu. Rev. Clin. Psychol. 9, 177–213.

Mitelman, S.A., Buchsbaum, M.S., 2007. Very poor outcome schizophrenia: clinical and neuroimaging aspects. Int. Rev. Psychiatry 19 (4), 345–357.

Moran, M.E., Hulshoff Pol, H., Gogtay, N., 2013. A family affair: brain abnormalities in siblings of patients with schizophrenia. Brain 136 (Pt 11), 3215–3226.

Pakkenberg, B., Gundersen, H.J., 1997. Neocortical neuron number in humans: effect of sex and age. J. Comp. Neurol. 384 (2), 312–320.

Pantev, C., 1995. Evoked and induced gamma-band activity of the human cortex. Brain Topogr. 7 (4), 321–330.

Papp, N., Ktonas, P., 1977. Critical evaluation of complex demodulation techniques for the quantification of bioelectrical activity. Biomed. Sci. Instrum. 13, 135–145.

Popov, T., Jordanov, T., Weisz, N., Elbert, T., Rockstroh, B., Miller, G.A., 2011. Evoked and induced oscillatory activity contributes to abnormal auditory sensory gating in schizophrenia. NeuroImage 56 (1), 307–314.

Rasetti, R., Weinberger, D.R., 2011. Intermediate phenotypes in psychiatric disorders. Curr. Opin. Genet. Dev. 21 (3), 340–348.

Rass, O., Forsyth, J.K., Krishnan, G.P., Hetrick, W.P., Klaunig, M.J., Breier, A., et al., 2012. Auditory steady state response in the schizophrenia, first-degree relatives, and schizotypal personality disorder. Schizophr. Res. 136 (1–3), 143–149.

Raz, N., Rodrigue, K.M., 2006. Differential aging of the brain: patterns, cognitive correlates and modifiers. Neurosci. Biobehav. Rev. 30 (6), 730–748.

Raznahan, A., Greenstein, D., Lee, Y., Long, R., Clasen, L., Gochman, P., et al., 2011. Catechol-o-methyl transferase (COMT) val158met polymorphism and adolescent cortical development in patients with childhood-onset schizophrenia, their non-psychotic siblings, and healthy controls. NeuroImage 57 (4), 1517–1523.

Roach, B.J., Mathalon, D.H., 2008. Event-related EEG time–frequency analysis: an overview of measures and an analysis of early gamma band phase locking in schizophrenia. Schizophr. Bull. 34 (5), 907–926.

Roberts, T.P., Khan, S.Y., Blaskey, L., Dell, J., Levy, S.E., Zarnow, D.M., et al., 2009. Developmental correlation of diffusion anisotropy with auditory-evoked response. Neuroreport 20 (18), 1586–1591.

Rosburg, T., Boutros, N.N., Ford, J.M., 2008. Reduced auditory evoked potential component N100 in schizophrenia—a critical review. Psychiatry Res. 161 (3), 259–274.

Rose, E.J., Donohoe, G., 2013. Brain vs behavior: an effect size comparison of neuroimaging and cognitive studies of genetic risk for schizophrenia. Schizophr. Bull. 39 (3), 518–526.

Salisbury, D.F., Kuroki, N., Kasai, K., Shenton, M.E., McCarley, R.W., 2007. Progressive and interrelated functional and structural evidence of post-onset brain reduction in schizophrenia. Arch. Gen. Psychiatry 64 (5), 521–529.

Selemon, L.D., Goldman-Rakic, P.S., 1999. The reduced neuropil hypothesis: a circuit based model of schizophrenia. Biol. Psychiatry 45 (1), 17–25.

Shenton, M.E., Dickey, C.C., Frumin, M., McCarley, R.W., 2001. A review of MRI findings in schizophrenia. Schizophr. Res. 49 (1–2), 1–52.

Smiley, J.F., Rosoklija, G., Mancevski, B., Mann, J.J., Dwork, A.J., Javitt, D.C., 2009. Altered volume and hemispheric asymmetry of the superficial cortical layers in the schizophrenia planum temporale. Eur. J. Neurosci. 30 (3), 449–463.

Smith, A.K., Edgar, J.C., Huang, M., Lu, B.Y., Thoma, R.J., Hanlon, F.M., et al., 2010. Cognitive abilities and 50- and 100-msec paired-click processes in schizophrenia. Am. J. Psychiatry 167 (10), 1264–1275.

Soros, P., Michael, N., Tollkotter, M., Pfleiderer, B., 2006. The neurochemical basis of human cortical auditory processing: combining proton magnetic resonance spectroscopy and magnetoencephalography. BMC Biol. 4, 25.

Spencer, K.M., Salisbury, D.F., Shenton, M.E., McCarley, R.W., 2008. Gamma-band auditory steady-state responses are impaired in first episode psychosis. Biol. Psychiatry 64 (5), 369–375.

Spencer, K.M., Niznikiewicz, M.A., Nestor, P.G., Shenton, M.E., McCarley, R.W., 2009. Left auditory cortex gamma synchronization and auditory hallucination symptoms in schizophrenia. BMC Neurosci. 10, 85.

Stark, A.K., Uylings, H.B., Sanz-Arigita, E., Pakkenberg, B., 2004. Glial cell loss in the anterior cingulate cortex, a subregion of the prefrontal cortex, in subjects with schizophrenia. Am. J. Psychiatry 161 (5), 882–888.

Steen, R.G., Mull, C., McClure, R., Hamer, R.M., Lieberman, J.A., 2006. Brain volume in first-episode schizophrenia: systematic review and meta-analysis of magnetic resonance imaging studies. Br. J. Psychiatry 188, 510–518.

Sweet, R.A., Pierri, J.N., Auh, S., Sampson, A.R., Lewis, D.A., 2003. Reduced pyramidal cell somal volume in auditory association cortex of subjects with schizophrenia. Neuropsychopharmacology 28 (3), 599–609.

Sweet, R.A., Bergen, S.E., Sun, Z., Sampson, A.R., Pierri, J.N., Lewis, D.A., 2004. Pyramidal cell size reduction in schizophrenia: evidence for involvement of auditory feedforward circuits. Biol. Psychiatry 55 (12), 1128–1137.

Sweet, R.A., Bergen, S.E., Sun, Z., Marcsisin, M.J., Sampson, A.R., Lewis, D.A., 2007. Anatomical evidence of impaired feedforward auditory processing in schizophrenia. Biol. Psychiatry 61 (7), 854–864.

Sweet, R.A., Henteleff, R.A., Zhang, W., Sampson, A.R., Lewis, D.A., 2009. Reduced dendritic spine density in auditory cortex of subjects with schizophrenia. Neuropsychopharmacology 34 (2), 374–389.

Taulu, S., Kajola, M., Simola, J., 2004. Suppression of interference and artifacts by the signal space separation method. Brain Topogr. 16 (4), 269–275.

Teale, P., Collins, D., Maharajh, K., Rojas, D.C., Kronberg, E., Reite, M., 2008. Cortical source estimates of gamma band amplitude and phase are different in schizophrenia. NeuroImage 42 (4), 1481–1489.

Turetsky, B.I., Greenwood, T.A., Olincy, A., Radant, A.D., Braff, D.L., Cadenhead, K.S., et al., 2008. Abnormal auditory N100 amplitude: a heritable endophenotype in first-degree relatives of schizophrenia probands. Biol. Psychiatry 64 (12), 1051–1059.

Winkler, A.M., Kochunov, P., Blangero, J., Almasy, L., Zilles, K., Fox, P.T., et al., 2010. Cortical thickness or grey matter volume? The importance of selecting the phenotype for imaging genetics studies. NeuroImage 53 (3), 1135–1146.